How to cite: *Angew. Chem. Int. Ed.* **2024**, *63*, e202316131
doi.org/10.1002/anie.202316131

VIP Microdroplet Chemistry Very Important Paper

Superfast Formation of C(sp^2)–N, C(sp^2)–P, and C(sp^2)–S Vinylic Bonds in Water Microdroplets

Yifan Meng, Richard N. Zare, and Elumalai Gnanamani**

Abstract: We report examples of C(sp^2)–N, C(sp^2)–S, and C(sp^2)–P bond-forming transformations in water microdroplets at room temperature and atmospheric pressure using N_2 as a nebulizing gas. When an aqueous solution of vinylic acid and amine is electrosprayed (+ 3 kV), the corresponding C(sp^2)–N product is formed in a single step, which was characterized using mass spectrometry (MS) and tandem mass spectrometry (MS^2). The scope of this reaction was extended to other amines and other unsaturated acids, including acrylic (CH_2=CHCOOH) and crotonic (CH_3CH=CHCOOH) acids. We also found that thiols and phosphines are viable nucleophiles, and the corresponding C(sp^2)–S and C(sp^2)–P products are observed in positive ion mode using MS and MS^2.

Vinylic C(sp^2)–N bond-forming reactions are important transformations in organic chemistry, and vinylic C(sp^2)–N motifs appear in several natural products and bioactive compounds.[1–5] For example, the botryllamides—which are ABCG2 inhibitors—contain an enamide and isolated from marine sediment-derived fungus.[3] Also, Erythrina alkaloid crystamidine, contains the C(sp^2)–N core, and it act as antagonizing the nicotinic acetyl choline receptor (nAChR),[4] as do several other natural products (Figure S1). Similarly, vinylic C(sp^2)–S and vinylic C(sp^2)–P moieties are also present in many medicinally important compounds, metal complexes, catalysts and building blocks in organic molecules synthesis.[6–11] For example, C(sp^2)–S (vinyl sulfone) motif containing molecule acts a neuroprotective agent for Parkinson's disease therapy.[11]

There are few methods available in the literature to synthesize products containing the vinylic C(sp^2)–N bond. Although the formation of C(sp^2)–N bonds is well-precedented for aromatic systems, methods for preparing vinyl amines are less common. These products have been prepared via Ru-catalyzed hydroamination of terminal alkynes and by Cu- and Pd-catalyzed couplings between functionalized vinyl compounds and amines, but other methods for accessing them are scarce.[12–17] Furthermore, methods for achieving the analogous C(sp^2)–S and C-(sp^2)–P bond formations are even less common. While these transformations are known, they require metal catalysts, high temperatures, or long synthetic sequences.[18–25] To the best of our knowledge, no report exists of achieving C(sp^2)–N, C(sp^2)–S, and C(sp^2)–P bond formations via the decarboxylation of vinylic acids. We present examples of all three processes promoted by water microdroplets at room temperature.

Our group and others have shown the use of microdroplets to accelerate reactions and obtain unexpected products.[26–39] Recent computational work by Colussi on the formation of hydroxyl and hydrogen radicals in water microdroplets helps explain the interesting catalytic properties of these systems, and clearly show that reactions in microdroplets occur via a radical-ionic cascade of reactions.[40] We recently developed a synthesis of hydrogen peroxide using water microdroplets and demonstrated that the hydroxyl radicals were stabilized on the air–water interface.[41] Additionally, recent studies explain that hydroxyl radical also forms at the surface of corona bubbles.[42] Furthermore, we leveraged this reactivity to perform catalyst-free functionalization of both benzoic acids (via decarboxylation) and methylbenzenes (via C–H activation).[43,44] In our efforts to further expand the utility of water microdroplet chemistry, we disclose here a decarboxylative coupling of vinylic acids with N-, S-, and P-centered nucleophiles. As with our previous work, these transformations occur under mild, catalyst-free conditions which are made to happen and accelerated by water microdroplets.

Figure 1 presents a schematic diagram of a typical microdroplet experiment. Vinylic acid (20 μM) was dissolved in a 9:1 (v:v) water/methanol solution. The

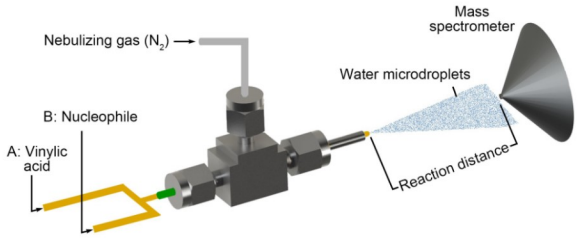

Figure 1. Schematic diagram of the water microdroplet experiment to form vinylic C(sp^2)–N, C(sp^2)–S, and C(sp^2)–P products.

[*] Y. Meng, R. N. Zare
Department of Chemistry, Stanford University
Stanford, CA 94305 (USA)
E-mail: zare@stanford.edu

E. Gnanamani
Department of Chemistry, Indian Institute of Technology Roorkee
Roorkee, 247667 (India)
E-mail: gnanam@cy.iitr.ac.in

purpose of adding methanol is to promote dissolution of vinylic acid in water. The result is similar when we added acetone to the water microdroplet instead of methanol. A dual-channel injection capillary (O.D. 350 μm, I.D. 70 μm) was used in this study to carry out the experiments, which enhanced the mixing of the two reactants. The solution containing vinylic acid was injected into the sprayer via channel A by a syringe pump with an injection speed of 5 μL/min. At the same time, a nucleophile (Nu), such as amine, was dissolved in water and injected through channel B at the same concentration of 20 μM and flow rate of 5 μL/min. Then, vinylic acid and Nu were mixed in the injection capillary. Acting as the nebulizing gas, N_2 (120 psi, 99.999 % purity) was used to generate water microdroplets. A positive voltage (3 kV) is applied to the microdroplet sprayer. Our previous study has shown that hydroxyl radicals are able to form without any external voltage. The purpose of applying a high voltage is to obtain a higher electric field at the water-gas surface to accelerate the rate of reaction (Figure S2). A high-resolution mass spectrometer (Orbitrap Velos Pro, Thermo Fisher Scientific, Waltham, MA) was used to detect the chemical components in water microdroplets. The distance between the microdroplet sprayer and the mass spectrometer inlet is defined as the reaction distance, which was maintained at 15 mm.

Cinnamic acid (vinylic acid) and propylamine (Nu) were used as model reagents to demonstrate the direct C–N bonding formation in water microdroplets. Figure 2A shows the reaction scheme of one-step-forming *N*-(2-phenylethenyl)-1-propanamine from cinnamic acid and propylamine. First, cinnamic acid was dissolved in a 9:1 (v:v) water/methanol solution and injected to the sprayer from channel A, while pure water was injected from channel B. Figure 2B shows the mass spectrum of water microdroplets that only contained cinnamic acid. The peak at *m/z* 103.0538 was identified to be vinylic carbocation (2-phenylethen-1-ylium, $C_8H_7^+$), whose exact *m/z* is 103.0542. Though the vinyl carbocations are unstable nature, we were able to detect and stabilize the vinylic carbocation intermediate ($C_8H_7^+$) in water microdroplets. Figure 2C shows the MS^2 spectrum of the peak at *m/z* 103.0538 shown in Figure 2B. We observed the peak at *m/z* of 77.0384, which is the phenyl cation ($C_6H_5^+$), a fragment from the collision-induced dissociation (CID) of $C_8H_7^+$. These results clearly prove the decarboxylation of cinnamic acid occurred in water microdroplets to form the vinylic carbocation intermediate. Figure 2D shows the intensity changes of vinylic cation ($C_8H_7^+$) and protonated product ($C_{11}H_{15}N^+$) before and after adding propylamine to the microdroplets. In this experiment, we first injected cinnamic acid and water from channel A and B from 0 to 0.5 min. As shown, during this period, the signal of $C_8H_7^+$ can be clearly observed and the intensity is maintained at a high level. Then propylamine was dissolved in water and injected from channel B from 0.5 to 1 min, while cinnamic acid is still injected from channel A. As shown from 0.5 to 1 minute, an obvious decrease in the signal intensity of vinylic carbocation ($C_8H_7^+$) occurred. Meanwhile, the product peak can be clearly detected. This result indicated that the vinylic cation participated in a chemical reaction as a reactant. It is worth to mention that the introduction of propylamine, which has a higher high proton affinity, can also lead to suppression of the vinylic cation intensity. Figure 2E shows the mass spectrum of protonated *N*-(2-phenylethenyl)-1-propanamine, which is the C–N bonding product in water microdroplets containing cinnamic acid and propylamine. The peak at *m/z* 162.1276 was identified to be protonated *N*-(2-phenylethenyl)-1-propanamine, whose formula is $[C_{11}H_{17}N+H]^+$. Figure 2F demonstrates the MS^2 spectrum of the product peak at *m/z* 162.1276

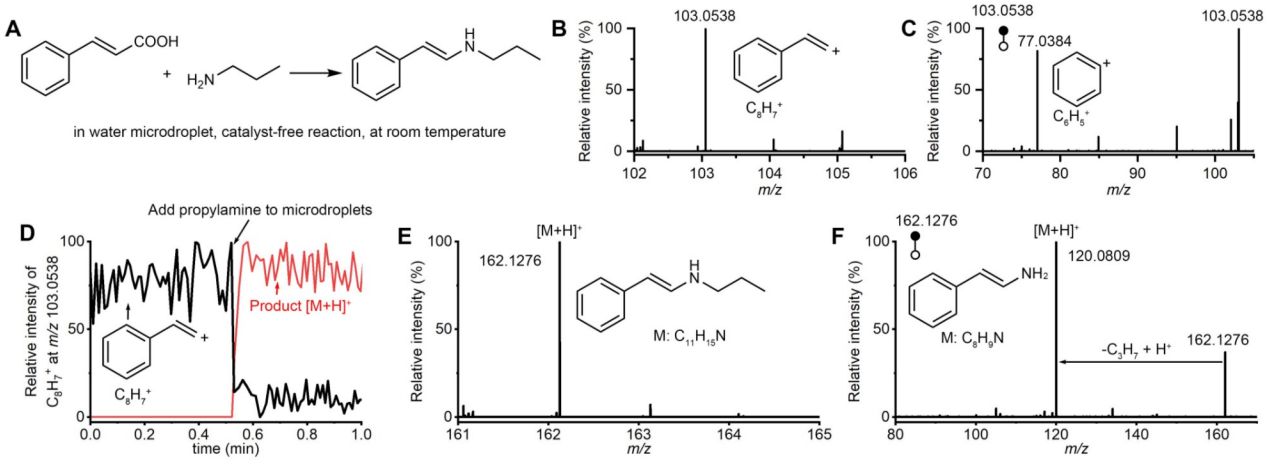

Figure 2. One-step C(sp^2)–N bond formation between cinnamic acid and propylamine in water microdroplets. (A) Reaction scheme for the decarboxylative formation of N-(2-phenylethenyl)-1-propanamine from cinnamic acid and propylamine in water microdroplets. (B) Mass spectrum of water microdroplets containing cinnamic acid. (C) MS^2 spectrum of the peak at *m/z* 103.0538 shown in panel (B). (D) Intensity changes of vinylic carbocation ($C_8H_7^+$) before and after adding propylamine to the microdroplets. (E) Mass spectrum of water microdroplets containing cinnamic acid and propylamine. (F) MS^2 spectrum of the peak at *m/z* 162.1276 shown in panel (E).

shown in Figure 2E. The fragment peak at *m/z* 120.0809 is from the CID of $C_{11}H_{15}N^+$. These results directly confirm the C–N bond formation between cinnamic acid and propylamine in water microdroplets. By monitoring the MS signal intensity of deprotonated cinnamic acid in negative ion mode with and without the addition of propylamine, we calculated that the conversion rate of cinnamic acid is about 14.9 % (Figure S3). As mentioned above, in the microdroplet experiment, the distance between the sprayer and the MS inlet was maintained at 15 mm. Our previous study showed that the jet velocity of the microdroplets generated by the sprayer is about 83 m/s while the nebulizing gas pressure is 120 psi.[45] Therefore, the reaction time can be calculated to be about 180 µs. This result indicates that the decarboxylative C–N bond formation between cinnamic acid and propylamine can be achieved in water microdroplets in less than 200 µs, which cannot occur in bulk water. The reaction speed in water microdroplets is multiple fold higher than other reactions reported for forming vinyl amines in bulk conditions.[13,17] By changing the reaction distance, we can see that the relative intensity of the product increased while increasing the reaction time from 50 to 200 µs (Figure S4).

Based on the results above, the mechanism for the formation of N-(2-phenylethenyl)-1-propanamine from cinnamic acid and propylamine in water microdroplets is proposed in Figure 3. As our group and others determined earlier, hydroxyl radicals form from water at the air–water interface and on corona bubbles[38] causing radical cleavage of the cinnamic acid to form the cinnamate radical. The cinnamate radical **II** further liberates CO_2 to form a vinylic radical **III**, which loses an electron to form a vinyl carbocation **IV**, which has been identified in positive ion mode of the mass spectrum (*m/z* 103.0538), as shown in Figure 2B. Trapping of this cation with the amine then gives rise to the C(sp^2)–N product **V**, observed at *m/z* 162.1276 (Figure 2E). To develop support for the reaction pathway, we carried out a control experiment using the radical scavenger 2,2,6,6-tetramethylpiperidin-1-yl)oxyl (TEMPO). We observed the marginal decrease of the C–N bond formation product, when adding 4 equivalents of TEMPO (Figure S5). Without TEMPO the intensity of product formation was higher and by increasing the concentration of TEMPO, the C–N bond formation gradually decreased. This result clearly indicates the reaction proceeds via radical intermediates. An analogous mechanism can be used to explain the formation of C(sp^2)–S and C(sp^2)–P adducts.

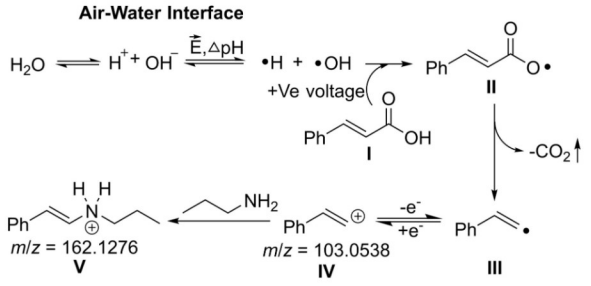

Figure 3. Proposed mechanism for forming N-(2-phenylethenyl)-1-propanamine from cinnamic acid and propylamine in water microdroplets.

By using the same method, we also explored the formation of C(sp^2)–N bond between other vinylic acids and amines in water microdroplets. In these experiments, the vinylic acids were also dissolved in a 9:1 solution of water and methanol and the concentration of each acid was adjusted to be 20 µM. The vinylic acid solution was injected from channel A with the same speed (5 µL/min). At the same time, amines (20 µM) were dissolved in water and injected from channel B. After mixing in the pure silica capillary, the microdroplets containing vinylic acid and amine were electrosprayed. To expand the scope of the reaction, we screened the reaction between cinnamic acid with other secondary and benzyl amine, and the corresponding C–N bond formation products were observed. Also, we further extended this work to aliphatic acids such as acrylic, crotonic, and 2-hexenoic acid. Figures 4A to 4F show the mass spectrum of water microdroplets containing cinnamic acid and diethylamine, cinnamic acid and benzylamine, cinnamic acid and pyrrolidine, 2-hexenoic acid and propylamine, crotonic acid and propylamine, and acrylic acid and propylamine, respectively. The peaks at *m/z* of 176.1441, 210.1281, 174.1278, 128.1438, 100.1116, and 86.0962 are identified to be the corresponding C–N bond formation products, whose molecular structural formula are shown next to each peak. The MS^2 spectra of the C–N bond formation products are shown in Figures S6–S10, which further verified the reaction between vinylic acids and amines in water microdroplets.

Inspired by the above reactions between vinylic acids and amines, we expanded the reaction to other nucleophiles, such as thiols and phosphines. First, we injected crotonic acid from channel A and ethanethiol from channel B. The chemical components of microdroplets generated by the sprayer were detected by mass spectrometry. Figure 5A shows the mass spectrum of water microdroplets containing crotonic acid and ethanethiol. The peak at *m/z* of 103.0578 is identified to be protonated vinyl sulfide (ethyl-1-propenylsulfide), whose formula is $C_5H_{11}S^+$. This product directly forms from the reaction between the vinyl carbocation ($C_3H_5^+$) and ethanethiol nucleophile. Figure 5B shows the MS^2 spectrum of the peak at *m/z* 103.0578 shown in Figure 5A. The peak at *m/z* of 75.0621 represents the fragment $C_3H_7S^+$ from the CID of the parent peak of $C_5H_{11}S^+$. The MS^2 data clearly indicates the C(sp^2)–S bond formation, between vinylic acid and thiols. We also carried out the water microdroplets containing cinnamic acid and benzyl mercaptan. The corresponding C–S bond formation product was observed at *m/z* 227.0886 in water microdroplets under mild conditions (Figure S11). In addition, we also observed $C_7H_7^+$ at *m/z* 91.0539 and $C_8H_9S^+$ at *m/z* 137.0358, which are identified to be fragments from the CID of the parent peak (Figure S12).

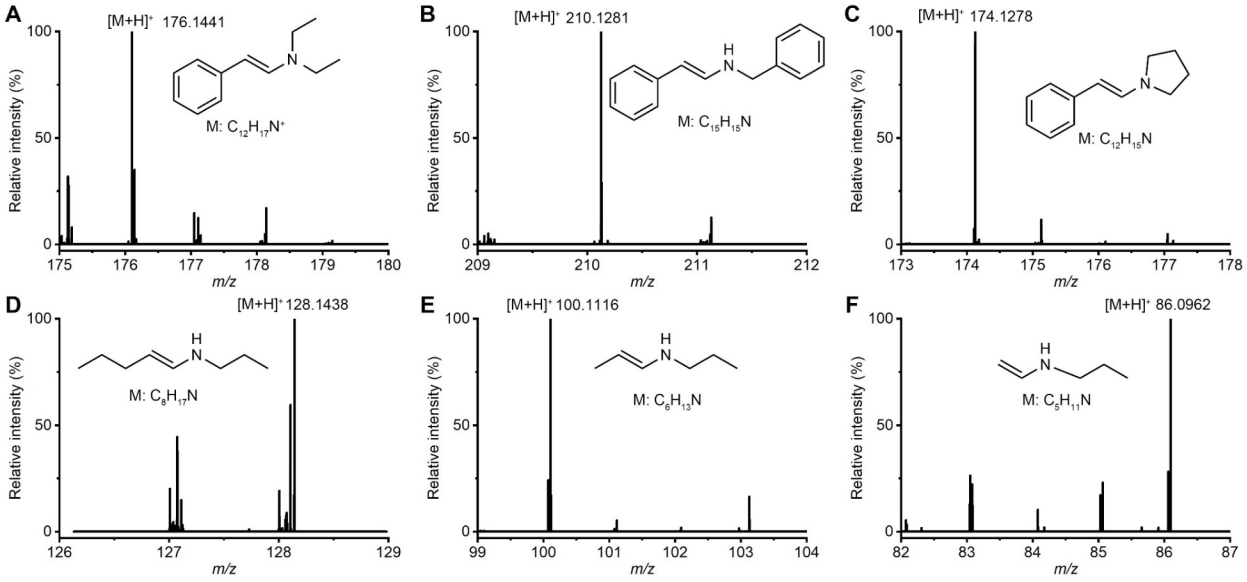

Figure 4. Formation of the C(sp^2)–N bond between other vinylic acids and amines in water microdroplets. Mass spectrum of water microdroplets containing (A) cinnamic acid and diethylamine, (B) cinnamic acid and benzylamine, (C) cinnamic acid and pyrrolidine, (D) 2-hexenoic acid and propylamine, (E) crotonic acid and propylamine, and (F) acrylic acid and propylamine.

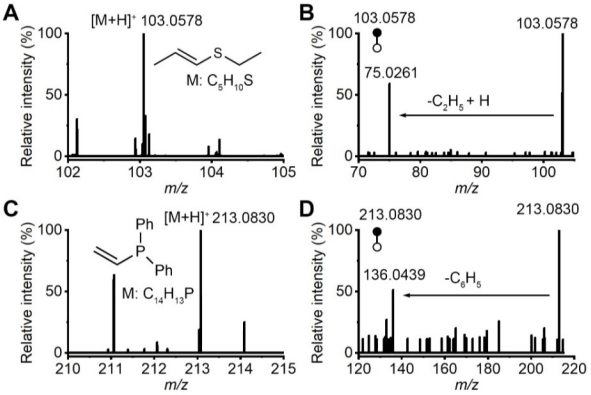

Figure 5. One-step C(sp^2)–S and C(sp^2)–P bond formation between vinylic acid and thiols and phosphines in water microdroplets. (A) Mass spectrum of water microdroplets containing crotonic acid and ethanethiol. (B) MS^2 spectrum of the peak at *m/z* 103.0578 shown in panel (A). (C) Mass spectrum of water microdroplets containing acrylic acid and diphenylphosphine. (D) MS^2 spectrum of the peak at m/z 213.0830 shown in panel (C).

The scope of the reaction methodology was further extended to the synthesis of the organophosphorus compound (vinyldiphenylphosphine). Generally, the vinylphosphines were synthesized from the reaction between chlorodiphenylphosphine and vinyl Grignard reagents.[46–48] The existing methods require a metal reagent or multiple steps. For the C(sp^2)–P bond formation experiment, diphenylphosphine was used as the nucleophile, and acrylic acid was used as the vinylic acid. Figure 5C shows the mass spectrum of water microdroplets containing acrylic acid and diphenylphosphine. The reaction was carried out at room temperature. The peak at *m/z* of 213.0380 represents the protonated C(sp^2)–P bond formation product (vinyldiphenylphosphine), whose molecular structure is shown in the Figure. Figure 5D shows the MS^2 spectrum of the peak at *m/z* 213.0830 shown in Figure 5C. The formation of product was confirmed by MS^2 and the observed data consistent with reported literature.[47] This result further verified the formation of the product. Furthermore, we also found the oxidative product, whose formula is $C_{14}H_{13}OP$ (Figure S13). The protonated product can be detected at *m/z* of 229.0771 ($C_{14}H_{14}OP$) and the fragments can also be observed (Figure S14).

In summary, we demonstrate a water microdroplet-promoted decarboxylative coupling of vinylic acids with a variety of N-, S-, and P-centered nucleophiles. Both aryl and aliphatic group substituted vinylic acids were coupled with a variety of amines to form the corresponding vinylic C(sp^2)–N bond containing products. The proposed mechanism intermediates were clearly identified using MS analysis. Further investigation of this transformation revealed that it can be extended to C(sp^2)–S and C(sp^2)–P bond formation. In all the cases, products were unambiguously characterized using MS and MS^2 analysis. Our method provides multiple advantages over other methods for forming vinylic C(sp^2)-heteroatom bonds, including simple starting materials, mild reaction conditions, and the lack of the need to use transition metal catalysts.

Supporting Information

Effect of applied voltage; Conversion rate; Time-resolved MS result; Capture radicals with TEMPO; Detection of multiple products; MS^2 spectra of products

Author Contributions

Experiments were carried out by Y.M. and E.G. The manuscript was written by all authors.

Acknowledgements

Funding: This work is supported by the Air Force Office of Scientific Research through the Multidisciplinary University Research Initiative (MURI) program (AFOSR FA9550-21-1-0170). EG thank the SERB, India (SRG/2021/0019070) and IIT-Roorkee faculty initiation grant.

Conflict of Interest

The authors declare no conflict of interest.

Data Availability Statement

The data that support the findings of this study are available from the corresponding author upon reasonable request.

Keywords: C(sp^2)–N,P,S Bond Formation · Mass Spectrometry · Microdroplet Chemistry

[1] E. M. Beccalli, G. Broggini, M. Martinelli, S. Sottocornola, *Chem. Rev.* **2007**, *107*, 5318–5365.
[2] A. Correa, C. Bolm in *Amination and Formation of sp^2C–N Bonds* (Eds.: M. Taillefer, D. Ma), Springer Berlin Heidelberg, Berlin **2013**, pp. 55–85.
[3] C. J. Henrich, R. W. Robey, K. Takada, H. R. Bokesch, S. E. Bates, S. Shukla, S. V. Ambudkar, J. B. McMahon, K. R. Gustafson, *ACS Chem. Biol.* **2009**, *4*, 637–647.
[4] H. Umihara, T. Yoshino, J. Shimokawa, M. Kitamura, T. Fukuyama, *Angew. Chem. Int. Ed.* **2016**, *55*, 6915–6918.
[5] W. Xu, X. Cai, M. E. Jung, Y. Tang, *J. Am. Chem. Soc.* **2010**, *132*, 13604–13607.
[6] L. Rout, T. Punniyamurthy, *Coord. Chem. Rev.* **2021**, *431*, 213675.
[7] T. G. Ostapowicz, C. Merkens, M. Hölscher, J. Klankermayer, W. Leitner, *J. Am. Chem. Soc.* **2013**, *135*, 2104–2107.
[8] A. J. M. Miller, J. A. Labinger, J. E. Bercaw, *J. Am. Chem. Soc.* **2008**, *130*, 11874–11875.
[9] M. Itazaki, S. Katsube, M. Kamitani, H. Nakazawa, *Chem. Commun.* **2016**, *52*, 3163–3166.
[10] M. A. Bennett, J. Castro, A. J. Edwards, M. R. Kopp, E. Wenger, A. C. Willis, *Organometallics* **2001**, *20*, 980–989.
[11] S. Y. Woo, J. H. Kim, M. K. Moon, S.-H. Han, S. K. Yeon, J. W. Choi, B. K. Jang, H. J. Song, Y. G. Kang, J. W. Kim, J. Lee, D. J. Kim, O. Hwang, K. D. Park, *J. Med. Chem.* **2014**, *57*, 1473–1487.
[12] M. Arndt, K. S. M. Salih, A. Fromm, L. J. Goossen, F. Menges, G. Niedner-Schatteburg, *J. Am. Chem. Soc.* **2011**, *133*, 7428–7449.
[13] Y. Bolshan, R. A. Batey, *Angew. Chem. Int. Ed.* **2008**, *47*, 2109–2112.
[14] L. Jiang, G. E. Job, A. Klapars, S. L. Buchwald, *Org. Lett.* **2003**, *5*, 3667–3669.
[15] A. Klapars, K. R. Campos, C.-y. Chen, R. P. Volante, *Org. Lett.* **2005**, *7*, 1185–1188.
[16] L. N. Berntsen, T. N. Solvi, K. Sørnes, D. S. Wragg, A. H. Sandtorv, *Chem. Commun.* **2021**, *57*, 11851–11854.
[17] Y. Morimoto, T. Kochi, F. Kakiuchi, *J. Org. Chem.* **2021**, *86*, 13143–13152.
[18] M. S. Driver, J. F. Hartwig, *J. Am. Chem. Soc.* **1996**, *118*, 7217–7218.
[19] Z. Lian, B. N. Bhawal, P. Yu, B. Morandi, *Science* **2017**, *356*, 1059–1063.
[20] T. Delcaillau, A. Bismuto, Z. Lian, B. Morandi, *Angew. Chem. Int. Ed.* **2020**, *59*, 2110–2114.
[21] H. F. Piedra, M. Plaza, *Chem. Sci.* **2023**, *14*, 650–657.
[22] X.-T. Liu, X.-Y. Han, Y. Wu, Y.-Y. Sun, L. Gao, Z. Huang, Q.-W. Zhang, *J. Am. Chem. Soc.* **2021**, *143*, 11309–11316.
[23] V. A. Pollard, A. Young, R. McLellan, A. R. Kennedy, T. Tuttle, R. E. Mulvey, *Angew. Chem. Int. Ed.* **2019**, *58*, 12291–12296.
[24] Y. Li, L. Liu, D. Shan, F. Liang, S. Wang, L. Yu, J.-Q. Liu, Q. Wang, X. Shao, D. Zhu, *ACS Catal.* **2023**, *13*, 13474–13483.
[25] L. Ling, C. Hu, L. Long, X. Zhang, L. Zhao, L. L. Liu, H. Chen, M. Luo, X. Zeng, *Nat. Commun.* **2023**, *14*, 990.
[26] Y. Meng, E. Gnanamani, R. N. Zare, *J. Am. Chem. Soc.* **2023**, *145*, 7724–7728.
[27] Y. Meng, E. Gnanamani, R. N. Zare, *J. Am. Chem. Soc.* **2023**, *145*, 32–36.
[28] S. Banerjee, E. Gnanamani, X. Yan, R. N. Zare, *Analyst* **2017**, *142*, 1399–1402.
[29] X. Song, Y. Meng, R. N. Zare, *J. Am. Chem. Soc.* **2022**, *144*, 16744–16748.
[30] H. Nie, Z. Wei, L. Qiu, X. Chen, D. T. Holden, R. G. Cooks, *Chem. Sci.* **2020**, *11*, 2356–2361.
[31] L. Qiu, R. G. Cooks, *Angew. Chem. Int. Ed.* **2022**, *61*, e202210765.
[32] D. Zhang, X. Yuan, C. Gong, X. Zhang, *J. Am. Chem. Soc.* **2022**, *144*, 16184–16190.
[33] C. Gong, D. Li, X. Li, D. Zhang, D. Xing, L. Zhao, X. Yuan, X. Zhang, *J. Am. Chem. Soc.* **2022**, *144*, 3510–3516.
[34] S. Jin, H. Chen, X. Yuan, D. Xing, R. Wang, L. Zhao, D. Zhang, C. Gong, C. Zhu, X. Gao, Y. Chen, X. Zhang, *JACS Au* **2023**, *3*, 1563–1571.
[35] X. Yuan, D. Zhang, C. Liang, X. Zhang, *J. Am. Chem. Soc.* **2023**, *145*, 2800–2805.
[36] A. Nandy, A. Kumar, S. Mondal, D. Koner, S. Banerjee, *J. Am. Chem. Soc.* **2023**, *145*, 15674–15679.
[37] P. Basuri, L. E. Gonzalez, N. M. Morato, T. Pradeep, R. G. Cooks, *Chem. Sci.* **2020**, *11*, 12686–12694.
[38] Y. Liu, Q. Ge, T. Wang, R. Zhang, K. Li, K. Gong, L. Xie, W. Wang, L. Wang, W. You, X. Ruan, Z. Shi, J. Han, R. Wang, H. Fu, J. Chen, C. K. Chan, L. Zhang, *Chem* **2023**, https://doi.org/10.1016/j.chempr.2023.09.019.
[39] Q. Ge, Y. Liu, K. Li, L. Xie, X. Ruan, W. Wang, L. Wang, T. Wang, W. You, L. Zhang, *Angew. Chem. Int. Ed.* **2023**, *62*, e202304189.
[40] A. J. Colussi, *J. Am. Chem. Soc.* **2023**, *145*, 16315–16317.
[41] M. A. Mehrgardi, M. Mofidfar, R. N. Zare, *J. Am. Chem. Soc.* **2022**, *144*, 7606–7609.
[42] Y. B. Vogel, C. W. Evans, M. Belotti, L. Xu, I. C. Russell, L.-J. Yu, A. K. K. Fung, N. S. Hill, N. Darwish, V. R. Gonçales,

M. L. Coote, K. Swaminathan Iyer, S. Ciampi, *Nat. Commun.* **2020**, *11*, 6323.
[43] Y. Meng, R. N. Zare, E. Gnanamani, *J. Am. Chem. Soc.* **2023**, *145*, 19202–19206.
[44] Y. Meng, E. Gnanamani, R. N. Zare, *J. Am. Chem. Soc.* **2022**, *144*, 19709–19713.
[45] J. K. Lee, S. Kim, H. G. Nam, R. N. Zare, *Proc. Natl. Acad. Sci. USA* **2015**, *112*, 3898–3903.
[46] A. A. Mikhailine, M. I. Maishan, A. J. Lough, R. H. Morris, *J. Am. Chem. Soc.* **2012**, *134*, 12266–12280.
[47] C. E. Anderson, D. C. Apperley, A. S. Batsanov, P. W. Dyer, J. A. K. Howard, *Dalton Trans.* **2006**, 4134–4145.
[48] G. Hirata, H. Satomura, H. Kumagae, A. Shimizu, G. Onodera, M. Kimura, *Org. Lett.* **2017**, *19*, 6148–6151.

Manuscript received: October 24, 2023
Accepted manuscript online: December 20, 2023
Version of record online: January 8, 2024